

# Intramolecular vibrational energy redistribution and intermolecular energy transfer of benzene in supercritical CO<sub>2</sub>: measurements from the gas phase up to liquid densities

R. von Benten<sup>a</sup>, A. Charvat<sup>a</sup>, O. Link<sup>a</sup>, B. Abel<sup>a</sup>, D. Schwarzer<sup>b,\*</sup>

<sup>a</sup> *Institut für Physikalische Chemie der Universität Göttingen, Tammannstrasse 6, D-37077 Göttingen, Germany*

<sup>b</sup> *MPI für Biophysikalische Chemie, Am Faßberg 11, D-37077 Göttingen, Germany*

Received 29 July 2003

## Abstract

Femtosecond pump probe spectroscopy was employed to measure intramolecular vibrational energy redistribution (IVR) and intermolecular vibrational energy transfer (VET) of benzene in the gas phase and in supercritical (sc) CO<sub>2</sub>. We observe two IVR time scales the faster of which proceeds within  $\tau_{\text{IVR}}^{(1)} < 0.5$  ps. The slower IVR component has a time constant of  $\tau_{\text{IVR}}^{(2)} = (48 \pm 5)$  ps in the gas phase and in scCO<sub>2</sub> is accelerated by interactions with the solvent. At the highest CO<sub>2</sub> density it is reduced to  $\tau_{\text{IVR}}^{(2)} = (6 \pm 1)$  ps. The corresponding IVR rate constants show a similar density dependence as the VET rate constants. Model calculations suggest that both quantities correlate with the local CO<sub>2</sub> density in the immediate surrounding of the benzene molecule. © 2004 Elsevier B.V. All rights reserved.

## 1. Introduction

The flow of vibrational energy within a polyatomic molecule and its transfer to the surrounding medium are fundamental processes that govern chemical reactivity and reaction pathways in the gas phase and in solution [1,2]. Short pulse lasers can nowadays directly follow this flow of energy by exciting a specific vibrational motion and monitoring the transient response of the molecule that provides a good test for theoretical models or for convenient but unjustified conjectures and assumptions. One such conjecture is that IVR in solution is fast and another is that it is statistical. In the light of the many experimental findings for various molecules in the gas phase it appears that neither the fast nor the statistical character of the IVR process should be taken for granted [3]. The vibrational relaxation process in solution is even more complicated. However, there has been experimental evidence that mechanisms which dominate IVR in the gas phase survive to some extent in solution and in sev-

eral cases non statistical IVR can be found [1]. Recently, femtosecond (fs) IR-pump–UV-probe spectroscopy beside infrared absorption spectroscopy and anti-Stokes Raman spectroscopy, has become a powerful tool for studying the relaxation in overtones or combination modes of high frequency vibrations of organic molecules in solution [4–11]. With this technique, recently introduced by Crim et al. [4], changes in the electronic absorption spectrum after selective overtone excitation can be measured as the overall relaxation populates Franck–Condon (FC) active vibrational modes in the ground state. This aspect of IR/UV transient absorption spectroscopy makes the technique complementary to infrared absorption [12] and anti-Stokes Raman spectroscopy [13,14]. In comparison with the techniques above transient electronic absorption spectroscopy is to some extent selective like a double resonance technique since it probes the FC-active modes of the molecule, however, it is not as selective as infrared absorption spectroscopy or anti-Stokes Raman spectroscopy because it cannot distinguish between them.

During the past two decades benzene has occupied a central place in experimental studies of IVR [15]. In

\* Corresponding author. Fax: +49-551-201-1501.

E-mail address: [dswar@gwdg.de](mailto:dswar@gwdg.de) (D. Schwarzer).

particular, it has become the prototype for theoretical modeling of IVR at higher excitation energies and state densities [16]. The reference for IVR of benzene in the condensed phase is the isolated molecule. From frequency domain spectra in the first C–H stretching overtone region [15] it is known that the IVR process in the isolated molecule consists of at least two sequential steps, one on a femtosecond [17] and one on a 10–20 ps timescale [15,18]. The crucial question whether the situation is similar in solution is not easy to answer because the impact of the solvent on different timescales of IVR is expected to be different. While the ultrafast timescale above is probably hardly affected by collisions the environment will likely have an impact on the later timescales of IVR. Therefore the experimental answer may ultimately depend upon the particular experiment. In recent time-resolved IVR experiments on aromatic compounds in solution we found that the low frequency FC-active vibrational modes of benzene are populated within a few picoseconds [19]. It is tempting to attribute this process to the 10–20 ps component known from the gas phase which in solution is accelerated by interactions with the bath. In order to proof this conjecture and to investigate solvent assisted IVR in more detail in the present study we performed density dependent IVR experiments on benzene in supercritical (sc) CO<sub>2</sub>. Supercritical fluids offer an excellent opportunity to tune the bath density smoothly from gas like to liquid like. Only a very limited number of experiments have been reported in the literature in which IVR and/or VET of molecules in sc fluids was investigated [20–22]. Very recently the Kajimoto group studied IVR and VET of CH<sub>2</sub>I<sub>2</sub> in scCO<sub>2</sub> [23] and scXe [24]. These experiments, however, covered a reduced density range of only  $0.7 < \rho_{\text{red}} < 1.7$ , with  $\rho_{\text{red}} = \rho/\rho_c$  ( $\rho_c$  is the critical density), i.e., the true gas phase limit was not approached.

## 2. Experimental

Details of our experimental approach have been published elsewhere [1,5,6,10]. The main idea is that the initially excited non-stationary ‘states’ in the two quanta region of the C–H stretch vibration are FC-inactive, but as energy redistributes in the molecule, the population of isoenergetic (zeroth order) combination vibrations having quanta in the FC-active modes causes an *increase* in the absorption on the long wavelength wing of the electronic absorption spectrum. The limited number of FC-active modes of the molecules can be identified by resonance Raman and dispersed fluorescence experiments [10]. Subsequent intermolecular vibrational energy transfer to the surrounding solvent *decreases* the absorption again.

The Ti:sapphire oscillator/regenerative amplifier system (RGA) pumping two optical parametric amplifiers (TOPAS, LIGHT CONVERSION, and a home build non-collinear optical parametric amplifier, NOPA) and most of the experimental setup was the same as that used in similar, earlier experiments [9,10]. Briefly, half of the output energy of the RGA at 800 nm was used to operate the TOPAS and generate excitation pulses tuned to the first overtone of benzene CH-stretch vibrations at 1670 nm. The remaining 800 nm light was frequency doubled and used to pump the NOPA which after frequency doubling produced probe pulses at around 280 nm. The width of the cross correlation of pump and probe pulses was about 200 fs. Excitation and delayed probe pulses were focused ( $f = 200$  mm) and overlapped in the sample cell. For experiments at pressures below 50 bar we used a stainless steel cell with 2 mm fused silica windows and an optical path length of 20 mm. For pressures up to 1 kbar a high pressure cell equipped with sapphire windows (1–2 mm) with an optical path length of 2 mm was used. Both cells were designed for temperatures up to 480 K. The temperature was controlled by electrical heating elements and a thermocouple. The pressure (100–500 bar) was controlled with a pressure gage that was attached to a separate high pressure unit equipped with a mechanical spindle press (NOVA SWISS). The supercritical solution was exchanged between laser shots by a small magnetic stirrer inside the cell. The concentrations of benzene in scCO<sub>2</sub> was 0.2 M. Transient difference absorptions were measured at 1 kHz for a particular time delay (controlled with a translation stage, NEWPORT) until an acceptable signal-to-noise level was reached ( $\sim 8000$  shots).

## 3. Results and discussion

Fig. 1 shows the UV-absorption profiles recorded at 278 nm after IR-excitation of the first CH-stretch overtone in benzene at 1670 nm. All the signals are characterized by initial fast sub-picosecond and subsequent slower rises followed by even slower decays. The rise of the signal can be attributed to the population of FC-active vibrational modes due to IVR, whereas the decay corresponds to VET to the bath. Accordingly, the absorption profiles were analyzed with a model function of the form

$$S(t) \propto \exp\left(-\frac{t}{\tau_{\text{VET}}}\right) - \left[ A \cdot \exp\left(-\frac{t}{\tau_{\text{IVR}}^{(1)}}\right) + (1 - A) \exp\left(-\frac{t}{\tau_{\text{IVR}}^{(2)}}\right) \right], \quad (1)$$

which was convoluted with a Gaussian-shaped instrument response function. The presence of at least two

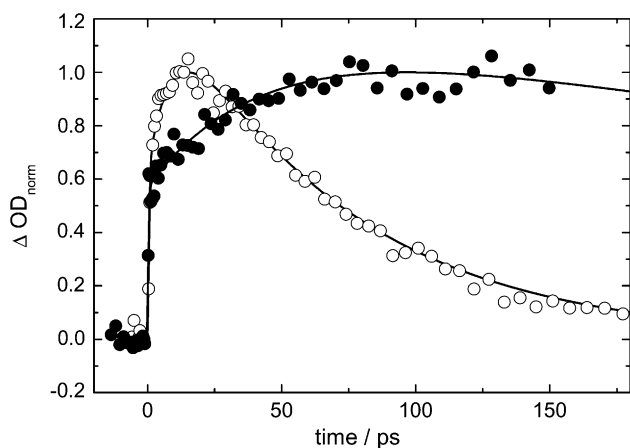


Fig. 1. Experimental traces for neat benzene in the gas phase (filled circles, 408 K, 4 bar) and in supercritical CO<sub>2</sub> (open circles, 100 bar, 318 K, 0.2 M concentration). The solid lines are fits of Eq. (1) (see text).

IVR-timescales is most clearly seen for the transient in Fig. 1 which was measured for neat gaseous benzene at 135 °C at the corresponding saturation pressure of about 4 bar (filled circles). Under these thermodynamic conditions the collision frequency is on the order of  $10^{10} \text{ s}^{-1}$ , i.e., the IVR process is measured nearly collision free and the time constants can be compared directly with those derived from eigenstate resolved spectra of benzene in the first C–H stretch overtone region. The fast IVR-component of the gas phase signal is below our time resolution such that we can only extract an upper limit of  $\tau_{\text{IVR}}^{(1)} < 0.5 \text{ ps}$ , whereas the slower one is characterized by a time constant of  $\tau_{\text{IVR}}^{(2)} = (48 \pm 5) \text{ ps}$ . The subsequent VET process takes place on a nano-second timescale and is not resolved. In order to fit the signal by means of Eq. (1) we calculated the VET time constant from the energy transfer data for benzene–benzene collisions derived by Barker and coworkers [25] to be  $\tau_{\text{VET}} = 0.6 \text{ ns}$  and used it as a fixed parameter.

Previous studies of benzene spectra at high resolution showed that the energy after C–H stretch overtone excitation is rapidly redistributed among a first tier of states within 100–200 fs. Dynamical calculations indicate that mainly high frequency modes containing pronounced in-plane C–H wagging and out-of-plane C–H bend character are responsible for this fast process [26,27]. Then, in a second, slower step taking 10–20 ps or even longer, further redistribution occurs into the low frequency ring modes of the molecule thus producing the linewidths and spectral features observed by Nicholson and Lawrence [18] and others [15]. The gas phase signal of Fig. 1 is in complete agreement with these observations. From analysis of the absorption spectrum it is known that the  $\nu_6$  ( $608 \text{ cm}^{-1}$ ) mode belongs to the FC-active mode responsible for hot band absorption at the benzene  $S_1 \leftarrow S_0$  electronic transition [28]. Theoretical studies have demonstrated that at 9.6 ps the relax-

ation into this mode is still incomplete [27]. Therefore, we tentatively attribute the slow IVR component of  $\tau_{\text{IVR}}^{(2)} = (48 \pm 5) \text{ ps}$  to the population of the  $\nu_6$  FC-active vibrational mode.

The open circles in Fig. 1 show an absorption signal of benzene in scCO<sub>2</sub> at a temperature of 45 °C and a pressure of 100 bar. Again, the transient is characterized by a fast initial rise of  $\tau_{\text{IVR}}^{(1)} < 0.5 \text{ ps}$ , but clearly, the following slower IVR and VET processes are accelerated with respect to the gas phase. Fitting of Eq. (1) to the signal by using the same amplitude ratio for slow and fast IVR component as in the gas phase (i.e.,  $A = 0.45$  in Eq. (1)) yields  $\tau_{\text{IVR}}^{(2)} = (9 \pm 1) \text{ ps}$  and  $\tau_{\text{VET}} = (68 \pm 7) \text{ ps}$  (if  $A$  were freely adjustable, our analysis yields  $A = 0.5 \pm 0.1$  and similar time constants indicating that  $A$  is density independent). These findings imply, that interactions with the surrounding not only reduce the VET time, but also can significantly enhance certain slow components of IVR. A pronounced density effect on IVR times for CH<sub>2</sub>I<sub>2</sub> dissolved in scXe was recently also observed by the Kajimoto group [24].

In Fig. 2 VET rate constants  $k_{\text{VET}} = 1/\tau_{\text{VET}}$  of benzene are plotted versus the CO<sub>2</sub> reduced density  $\rho_{\text{red}} = \rho/\rho_c$ , where  $\rho_c$  is the critical density of CO<sub>2</sub>.  $k_{\text{VET}}$  shows the same density dependence as observed previously for the vibrational energy relaxation of azulene in supercritical fluids [22,29]. The low density linear increase of  $k_{\text{VET}}(\rho)$  around the critical density slows down, before at about liquid densities it becomes stronger again. In our studies on azulene we have demonstrated that this behavior is governed by the local density and can be rationalized within the framework of the isolated binary collision model, where the deactivation rate of the excited molecule is proportional to the collision frequency  $Z(\rho, T)$ . Whilst  $Z$  in the gas phase linearly

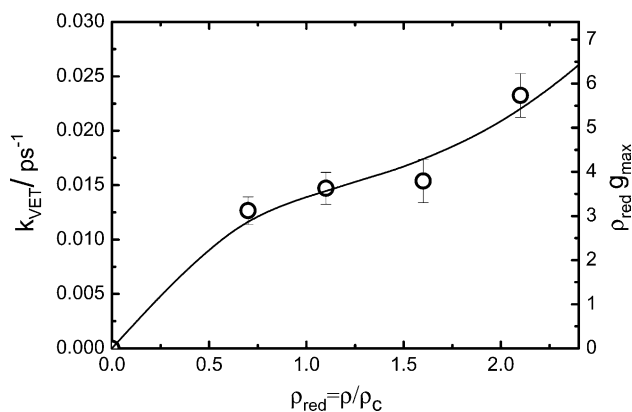


Fig. 2. VET rate constants of benzene in scCO<sub>2</sub> as a function of reduced density (open circles). Reduced densities, temperatures and pressures are:  $\rho_{\text{red}} = 2.1$  (500 bar, 318 K),  $\rho_{\text{red}} = 1.5$  (150 bar, 318 K),  $\rho_{\text{red}} = 1.2$  (100 bar, 318 K),  $\rho_{\text{red}} = 0.7$  (100 bar, 328 K). The solid line represents calculations of the local density at the position of the first maximum of the radial distribution function around an attractive solute in a Lennard-Jones fluid (see Fig. 4 and text for details).

depends on  $\rho$ , at higher density many-body effects lead to modifications of the pair distribution function  $g(r)$  around the solute giving rise to the characteristics observed in Fig. 2.

Inspection of the slower IVR rate constants  $k_{\text{IVR}}^{(2)} = 1/\tau_{\text{IVR}}^{(2)}$  of benzene in  $\text{scCO}_2$  indicates a very similar density dependence as found for  $k_{\text{VET}}(\rho)$ , see Fig. 3. Under nearly collision free conditions, i.e. at  $\rho \rightarrow 0$ ,  $k_{\text{IVR}}^{(2)}$  is given by anharmonic couplings intrinsically present in the benzene molecule. At higher densities interactions with the bath enhance these couplings and accelerate  $k_{\text{IVR}}^{(2)}$ . At the highest  $\text{CO}_2$  density the IVR process is characterized by a time constant of  $(6 \pm 1)$  ps which is already very close to 4 ps observed in a solvent like 1,1,2-trichlorotrifluoroethane [19]. We, however, do not observe a saturation of the solvent induced IVR rate at high density found for  $\text{CH}_2\text{I}_2$  in  $\text{scXe}$  [24]. Fig. 3 suggests that the IVR rate can be represented by a sum of the form

$$k_{\text{IVR}}^{(2)} = k_{\text{IVR}}^{\text{intra}} + k_{\text{IVR}}^{\text{inter}}, \quad (2)$$

where the rate constants  $k_{\text{IVR}}^{\text{intra}}$  and  $k_{\text{IVR}}^{\text{inter}}$  are influenced by intra- and intermolecular couplings, respectively. While  $k_{\text{IVR}}^{\text{intra}}$  is density independent,  $k_{\text{IVR}}^{\text{inter}}$  represents the density dependent part of  $k_{\text{IVR}}^{(2)}$ .

In an attempt to understand  $k_{\text{VET}}(\rho)$  and  $k_{\text{IVR}}^{(2)}(\rho)$  in more detail we calculated local densities from a simple model assuming benzene and  $\text{CO}_2$  to be Lennard-Jones particles and employing the (constant NVT) Monte Carlo method [30]. The solvent parameter  $\sigma_v$  and  $\varepsilon_v$  were chosen such that the critical data of the Lennard-Jones fluid [31] ( $T_c^* = k_B T_c / \varepsilon_v = 1.31$ ,  $\rho_c^* = \rho_c \sigma_v^3 = 0.31$ ) match those of  $\text{CO}_2$  ( $T_c = 304.13$  K,  $\rho_c = 10.6$  mol  $\text{l}^{-1}$ ), i.e.  $\sigma_v = 0.365$  nm and  $\varepsilon_v / k_B = 232.2$  K. For benzene we assumed an effective diameter of  $\sigma_u = 0.546$  nm which leads to  $\sigma = (\sigma_u + \sigma_v) / 2 = 0.456$  nm using standard combining rules. The well depth for the solute–solvent interactions represents the most sensitive parameter in these calculations and was adjusted to  $\varepsilon / k_B = 500$  K.

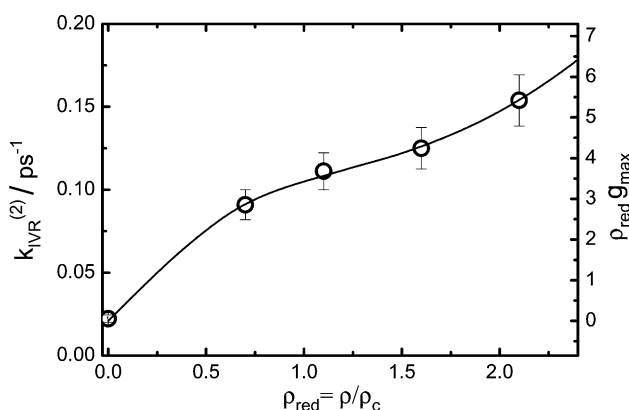


Fig. 3. Rate constants for the slow IVR component of benzene in the gas phase ( $\rho \rightarrow 0$ ) and in  $\text{scCO}_2$  (open circles); solid line: as Fig. 2, but shifted by  $k_{\text{IVR}}^{\text{intra}}$  see text.

The temperature was  $T = 318$  K; calculations were performed with 500 particles. Fig. 4 shows radial density distributions  $\rho_{\text{red}} \cdot g(r)$  around benzene for various bath densities derived from these simulations. The curves were obtained by constantly increasing the reduced density from  $\rho_{\text{red}} = 0.1613$  (lowest curve) to 2.581 (upper curve) in steps of 0.1613. Whereas at large distances ( $r/\sigma_v > 4$ ) all the distributions are separated by a constant value, this is not the case in the immediate surrounding of the solute represented by the first maximum  $\rho_{\text{red}} \cdot g_{\text{max}}$ . In fact, around the critical density (dashed line) the local density increases significantly slower than at lower or higher densities. In Figs. 2 and 3 the density dependence of  $\rho_{\text{red}} \cdot g_{\text{max}}$  is scaled in such a way, that it matches the experimental points, respectively. Additionally, the origin of the  $\rho_{\text{red}} \cdot g_{\text{max}}$  axis at the right side of Fig. 3 is shifted such that it coincides with  $k_{\text{IVR}}^{\text{intra}}$  at the left side. For both plots the agreement between model and experiment is very good considering the simplicity of the model.

Within the Landau–Teller approach the VET rate is proportional to the frequency dependent friction  $\xi(\omega)$  at the oscillator frequency  $\omega$ , calculated from the time-correlation function of the solvent forces acting on the vibrational coordinate of the solute [2,32,33]. The force components contributing to  $\xi(\omega)$  are known to be generated at the repulsive part of the solute–solvent interaction potential. Therefore,  $k_{\text{VET}}(\rho)$  depends on the local density at shorter distances than the position of  $g_{\text{max}}$  [34]. However, the local densities at both positions are strongly correlated and show similar density dependencies [35]. Hence  $\rho_{\text{red}} \cdot g_{\text{max}}$  can be taken as a measure of the collision frequency determining  $k_{\text{VET}}(\rho)$ . In the case of IVR it is not well understood how the solvent enhances the intramolecular couplings. We cannot unambiguously judge whether the solvent influ-

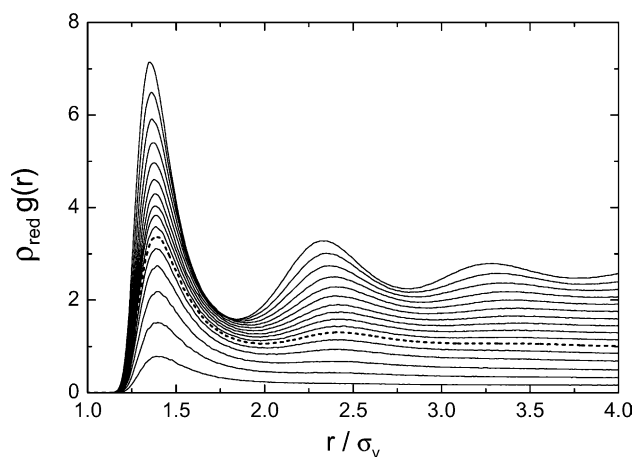


Fig. 4. Radial density distributions around an attractive Lennard-Jones particle (representing benzene) in a Lennard-Jones fluid (representing  $\text{CO}_2$ ) at reduced densities of  $\rho_{\text{red}} = 0.1613$  (lowest curve) to 2.581 (upper curve) in steps of 0.1613 (dashed line: closest to the critical density).

ence on  $k_{\text{IVR}}^{\text{inter}}$  is of more static character like the well known density dependent frequency shift of vibrational transitions, or is of more dynamic origin namely collisions, although at present we favor the picture of a collisionally enhanced process. However, no matter what the nature of the process is,  $k_{\text{IVR}}^{\text{inter}}$  clearly scales with the local density around the benzene molecule similar to the VET process. Further detailed insight into the nature of solvent induced IVR may be obtained from theoretical studies which are in progress at present.

### Acknowledgements

The authors thank the Deutsche Forschungsgemeinschaft for financial support within the Sonderforschungsbereich 357 ('Molekulare Mechanismen Unimolekularer Reaktionen'). We thank Dr. J. Aßmann and P. Kutne for help with the experimental setup. Financial support from the Fonds der Chemischen Industrie is also gratefully acknowledged.

### References

- [1] J. Aßmann, M. Kling, B. Abel, *Angew. Chem. Int. Ed.* 42 (2003) 2.
- [2] J.C. Owrutsky, D. Raftery, R.M. Hochstrasser, *Ann. Rev. Phys. Chem.* 45 (1994) 519.
- [3] D.J. Nesbitt, R.W. Field, *J. Phys. Chem.* 100 (1996) 12735.
- [4] D. Bingemann, A.M. King, F.F. Crim, *J. Chem. Phys.* 113 (2000) 5018.
- [5] A. Charvat, J. Aßmann, B. Abel, D. Schwarzer, *J. Phys. Chem. A* 105 (2001) 5071.
- [6] A. Charvat, J. Aßmann, B. Abel, D. Schwarzer, K. Henning, K. Luther, J. Troe, *Phys. Chem. Chem. Phys.* 3 (2001) 2230.
- [7] C.M. Cheatum, M.M. Heckscher, D. Bingemann, F.F. Crim, *J. Chem. Phys.* 115 (2001) 7086.
- [8] M.M. Heckscher, L. Sheps, D. Bingemann, F.F. Crim, *J. Chem. Phys.* 117 (2002) 8917.
- [9] J. Assmann, A. Charvat, D. Schwarzer, C. Kappel, K. Luther, B. Abel, *J. Phys. Chem. A* 106 (2002) 5197.
- [10] J. Assmann, R. von Benten, A. Charvat, B. Abel, *J. Phys. Chem. A* 107 (2003) 1904.
- [11] C.G. Elles, D. Bingemann, M.M. Heckscher, F.F. Crim, *J. Chem. Phys.* 118 (2003) 5587.
- [12] H.J. Bakker, P.C.M. Planken, A. Langendijk, *Nature* 347 (1990) 745.
- [13] L.K. Iwaki, J.C. Deak, S.T. Rhea, D.D. Dlott, *Chem. Phys. Lett.* 303 (1999) 176.
- [14] I. Hartl, W. Zinth, *J. Phys. Chem. A* 104 (2000) 4218.
- [15] A. Callegari, U. Merker, P. Engels, H.K. Srivastava, K.K. Lehmann, *J. Chem. Phys.* 113 (2000) 10583.
- [16] E.L. Siebert, W.P. Reinhardt, J.T. Hynes, *J. Chem. Phys.* 81 (1984) 1115.
- [17] R.H. Page, Y.R. Shen, Y.T. Lee, *J. Chem. Phys.* 88 (1987) 4621.
- [18] J.A. Nicholson, W.D. Lawrance, *Chem. Phys. Lett.* 236 (1995) 336.
- [19] R. von Benten, O. Link, B. Abel, D. Schwarzer, *J. Chem. Phys. A* 108 (2004) 363.
- [20] D.J. Myers, M. Shigeiwa, M.D. Fayer, *J. Phys. Chem. B* 104 (2000) 2402.
- [21] D. Schwarzer, J. Troe, M. Votsmeier, M. Zerezke, *J. Chem. Phys.* 105 (1996) 3121.
- [22] D. Schwarzer, J. Troe, M. Zerezke, *J. Chem. Phys.* 107 (1997) 8380.
- [23] K. Sekiguchi, A. Shimojima, O. Kajimoto, *Chem. Phys. Lett.* 356 (2002) 84.
- [24] K. Sekiguchi, A. Shimojima, O. Kajimoto, *Chem. Phys. Lett.* 370 (2003) 303.
- [25] B.M. Toselli, J.R. Barker, *J. Chem. Phys.* 97 (1992) 1809.
- [26] T.J. Minehardt, J.D. Adcock, R.E. Wyatt, *J. Chem. Phys.* 110 (1999) 3326.
- [27] T.J. Minehardt, J.D. Adcock, R.E. Wyatt, *Chem. Phys. Lett.* 303 (1999) 537.
- [28] J.H. Callomon, T.M. Dunn, I.M. Mills, *Phil. Trans. Roy. Soc. (London) A* 259 (1966) 499.
- [29] D. Schwarzer, J. Troe, M. Zerezke, *J. Phys. Chem. A* 102 (1998) 4207.
- [30] M.P. Allen, D.J. Tildesley, *Computer Simulation of Liquids*, Clarendon Press, Oxford, 1996.
- [31] J.J. Potoff, A.Z. Panagiotopoulos, *J. Chem. Phys.* 109 (1998) 10914.
- [32] L.D. Landau, E.A. Teller, *Phys. Z. Sowjetunion* 10 (1936) 34.
- [33] D.W. Oxtoby, *Adv. Chem. Phys.* 47 (1981) 487.
- [34] M. Teubner, D. Schwarzer, *J. Chem. Phys.* 119 (2003) 2171.
- [35] V.S. Vikhrenko, D. Schwarzer, J. Schroeder, *Phys. Chem. Chem. Phys.* 3 (2001) 1000.